

# GROUND DEMONSTRATION OF SYNCHRONIZED FORMATION ROTATIONS FOR PRECISION, MULTI-SPACECRAFT INTERFEROMETERS

Daniel P. Scharf, Jason A. Keim, and Fred Y. Hadaegh

Jet Propulsion Laboratory, California Institute of Technology, Pasadena, USA

## ABSTRACT

A major technology milestone for the Terrestrial Planet Finder Interferometer is the ground demonstration of precision, synchronized formation rotations. In a synchronized formation rotation the spacecraft move as if embedded in a virtual rigid body. This maneuver requires the highest control precision: the 6DOF flight requirements are to control inertial attitudes to  $\pm 1$  arcmin and relative positions to  $\pm 1$  cm. The requirements are inherently 6DOF because attitude motion is coordinated with relative translational motion. For ground demonstrations, the requirements are relaxed due to the increased disturbance environment to 6.6 arcmin RMS in attitude and 5 cm RMS in relative position.

This paper reports the ground demonstration of precision synchronized formation rotations with better than 6 arcmin/5 cm performance in the Formation Control Testbed (FCT). The FCT currently consists of two, five degree-of-freedom, air bearing-levitated robots. The sixth degree-of-freedom, vertical translation, is being added in November 2007. Each robot has a suite of flight-like avionics and actuators, including a star tracker, fiber-optic gyroscopes, reaction wheels, cold-gas thrusters, inter-robot communication, and on-board computers that run the Formation and Attitude Control System software.

After reviewing the relevant aspects of the FCT, the synchronized formation rotation maneuver is presented. Then the on-board guidance algorithm for autonomous maneuver execution is briefly presented, including an outer formation control loop that prevents the formation from drifting into the boundary of the operational area of the testbed. The main results of the paper are then given: six synchronized formation rotations with different guidance parameters to demonstrate algorithmic flexibility. The demonstrations occurred over two weeks to show a repeatable, robust capability.

Key words: Precision formation flying, Synchronized rotations, Ground testbed.

## 1. INTRODUCTION

Multi-spacecraft apertures are being studied for examining the atmospheres of terrestrial exo-planets in the infrared (Ref. 1, 2), observing the Earth with microwaves (Ref. 3), and imaging the event horizon of a black hole by means of X-ray emissions from in-

falling gas (Ref. 4). See (Ref. 5) for a list of over thirty multi-spacecraft missions.

Distributed spacecraft missions require varying levels of inter-spacecraft coupling. We define a *formation* as a group of separate spacecraft with a subset of dynamic states coupled by automatic feedback control such that a direct or indirect coupling exists between any pair of spacecraft. Essentially, if the state of one spacecraft changes unexpectedly, the other spacecraft react. When the spacecraft are coupled by only on-board sensor measurements, we refer to the group as a *knowledge formation*. Finally, if the spacecraft are controlled independently or from the ground and have no inter-spacecraft sensing, they are considered a *constellation*.

For planned and proposed formations, spacecraft separations range from meters to thousands of kilometers (Ref. 4, 6, 7). Spacecraft will need to autonomously maneuver over dynamic ranges of several orders-of-magnitude while minimizing and balancing fuel consumption, avoiding collision, and ensuring inter-spacecraft sensors remained locked (Ref. 8, 9).

Interferometric synthetic apertures also require spacecraft to autonomously perform precision, synchronized six degree-of-freedom (DOF) rotations. These 6DOF maneuvers simultaneously move the collecting apertures to sample the so-called  $u, v$ -plane while maintaining attitude alignment so that collected light can be routed to a combiner spacecraft. Since the interferometric payload is operating, these rotations also require the highest control precision: typically, on the order of 1 cm in at least one translational degree of freedom. Attitude requirements depend on the specific optical design of the payload and can vary from 1 arcmin down to 0.5 arcsec. For interferometry, adaptive optics then reduce the residual optical path length errors due to spacecraft motions down to the nanometer-level.

The technology roadmap for the Terrestrial Planet Finder Interferometer (TPF-I) (Ref. 10) identifies several key technology milestones. In particular, the Formation Control Testbed (FCT) will demonstrate at the system-level an autonomous formation rotation through 90 deg. with relative position control of  $\leq 5.0$  cm RMS and attitude control of  $\leq 6.67$  arcmin RMS. These requirements were derived from system-level error budgets for ground demonstrations of precision formation flying that account for the increased terrestrial disturbance environment. In addition, these requirements must be met three times



Figure 1. Formation Control Testbed Operations Area with Two Robots.

with at least two days between each demonstration. This temporal requirement ensures that the technology capability developed is robust and repeatable.

The primary contribution of this paper is to report the completion of the demonstration rotations and describe the experimental results. The technology roadmap milestone awaits confirmation by an independent review board in December 2007. The following section overviews the FCT. Next, the synchronized formation rotation maneuver is summarized as well as the on-board formation guidance algorithm for generating spacecraft trajectories. Then experimental results for the formation rotations are given. We conclude with near-term developments for the FCT and future directions.

## 2. FORMATION CONTROL TESTBED

The Formation Control Testbed (FCT) is a multi-robot, flight-like, system-level testbed for ground validation of formation GNC architectures and algorithms, including autonomous rendezvous and formation infrastructure technologies such as communication protocols and formation sensors (Ref. 11, 12). The FCT currently consists of two robots with flight-like hardware and dynamics, a precision flat floor that the robots operate on, ceiling-mounted artificial stars for attitude sensing and navigation, and a “ground control” room for remotely commanding the robots and receiving telemetry. A third robot is planned. The robots and part of the flat floor are shown in Figure 1. The FCT was designed and built in cooperation with industry partners Guidance Dynamics Corporation, Di-Tec International, and Applied Control Environments, Inc.

A detailed view of a robot with specific hardware identified is given in Figure 2. Each robot has a lower translational stage (TS) and an upper attitude stage (AS). The AS is the spacecraft emulator, and it is completely disconnected from the TS. The attitude stages are shown tilted in Figure 1. Each AS

houses avionics, spacecraft actuators, sensors, inter-robot and ground-to-robot communication antennas, and the spacecraft processors. With reference to Figure 2, the TS provides both translational and rotational degrees of freedom to the attitude stage by means of (i) linear air bearings that float an entire robot on a cushion of air a few thousandths of an inch thick, and (ii) a spherical air bearing in which a spherical surface on the bottom of the AS floats on a cushion of air generated in a pressurized cup at the top of the TS. A telescoping vertical stage with several tens-of-centimeters of travel is currently being installed to provide the translational degree of freedom normal to the flat floor. With the air bearings floated, the robot dynamics emulate deep space. Additionally, an outer, thruster control loop can add forces that emulate gravity gradients. The spherical air bearing allows full rotation of the AS about the axis normal to the flat floor and  $\pm 30$  deg. in the transverse axes.

The FCT is housed in the former Celestarium at JPL, which had been used to calibrate star trackers. As a result, the FCT has a 12.2 m-diameter floor space and a 7.6 m high, dome-like ceiling. See Figure 3. The 7.3 m x 8.5 m flat floor of the FCT consists of fourteen, 1.2 m x 3.7 m metal panels. Each panel is ground to a smoothness of a few thousandths of an inch and mounted on a support structure that has coarse and vernier leveling screws. Periodic laser surveys of the floor are used to level the floor panels and ensure the steps between them are no more than a few thousandths of an inch.

Each robot has an on-board PPC750 single board computer for the Formation and Attitude Control System (FACS) software (Ref. 13). All attitude and formation algorithms are run on-board; only commands are up-linked to the robots. The FACS is encapsulated by a Software Executive that provides a flight-like environment for execution and is designed to support a wide variety of control architectures and algorithms. An SE also provides command and telemetry handling, device-level communi-

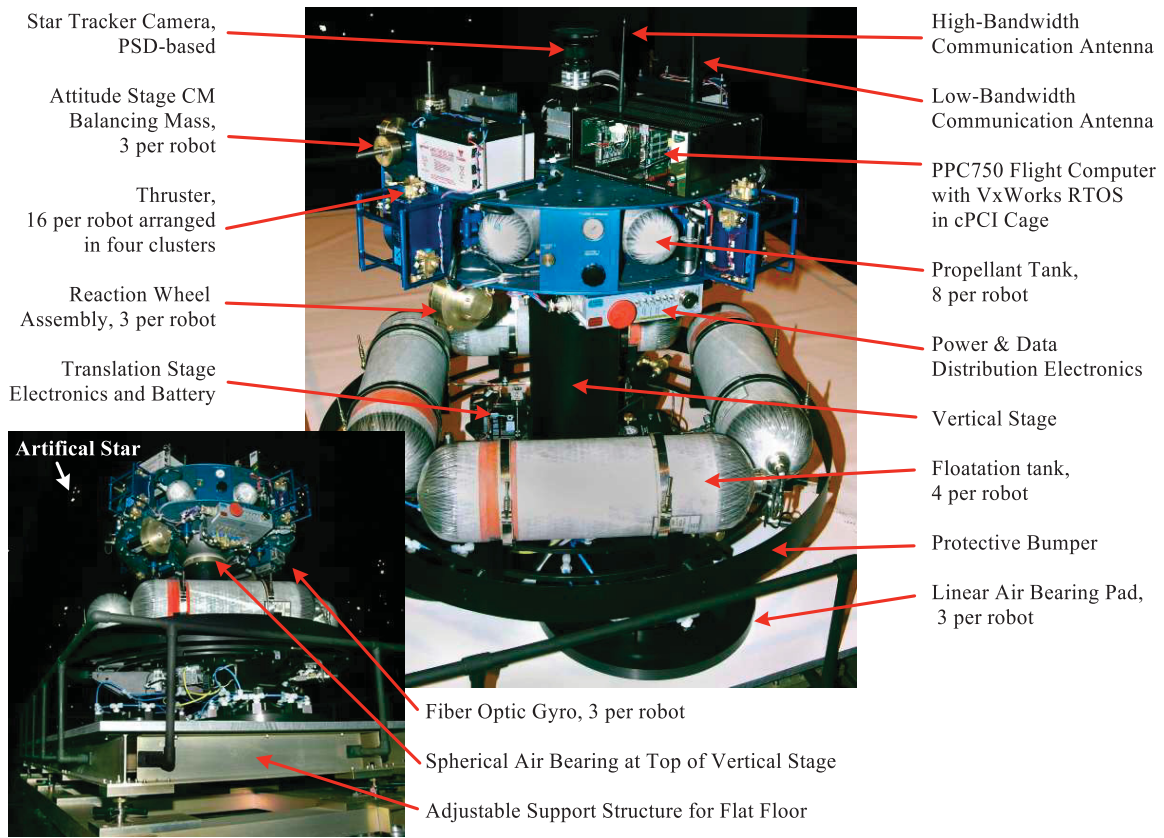


Figure 2. Major Components of an FCT Robot.

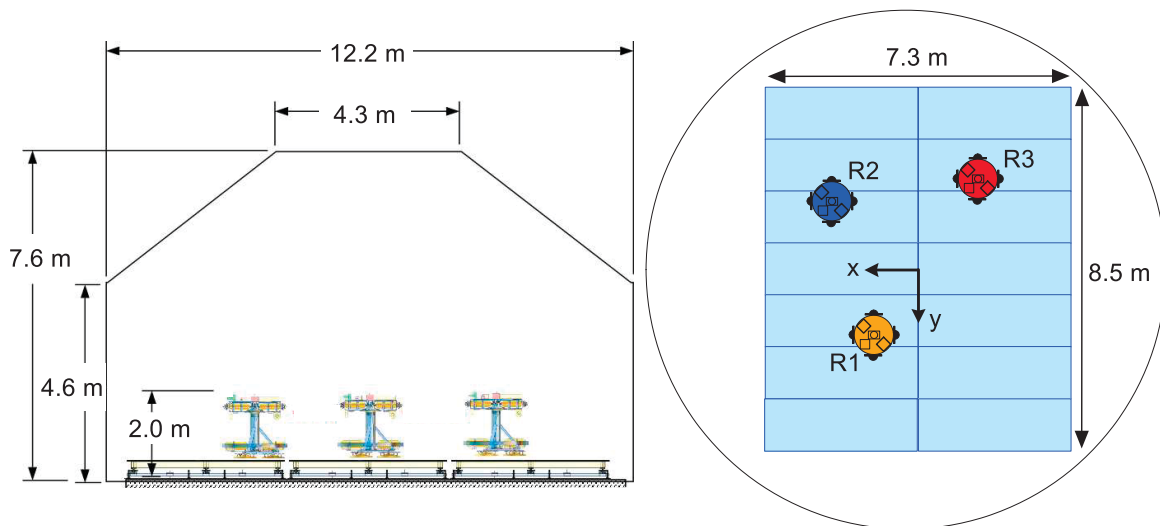


Figure 3. Side- and Top-View Schematics of the FCT Operational Area. Views show three robots to scale. Top-view also shows Room Frame origin, and  $x$ - and  $y$ -axes.

cation, inter-spacecraft communication, and scheduling within the real-time VxWorks operating system (Ref. 14).

The actuators on each robot consist of sixteen thrusters with 0.5-22 N thrust range arranged symmetrically in clusters of four and three, orthogonally-mounted reaction wheel assemblies (RWAs). The thrusters have a minimum on-time of 6 ms and a specific impulse of 55 s. Each wheel is capable of delivering 0.2 Nm and storing 1.4 Nms.

In addition to flight-like actuation and dynamics, each robot has typical, single-spacecraft attitude sensors and avionics. The attitude sensors consist of three, orthogonally-mounted KVH DSP-3000 fiber optic gyros and a pseudo-star tracker. The star tracker measures the directions to strobed, infra-red beacons that are mounted on the ceiling of the FCT and function as artificial stars. See Figure 4. Since the stars are in the near-field, the direction from a robot to the stars changes as the robot moves, thereby coupling attitude and position. By measuring the direction to three stars, the coupled position and attitude can be determined. The quaternion and position measurements are separated in the avionics and fed to the flight computer as the output of a star tracker and a GPS-like position sensor.

The FCT star trackers were calibrated with a Physik Instrumente M-85 hexapod, which has a 6DOF repeatability of  $\pm 2 \mu\text{m}$  and  $\pm 1$  arcsec in translation and rotation, respectively. For calibration, a laser surveyor was used to accurately determine the position and attitude of the hexapod in the FCT Room Frame. Then, a star tracker was translated and rotated on the hexapod to several poses as it was taking data. This data was used to fit Zernike polynomials for lens aberrations (Ref. 15). The per-axis, small angle standard deviations of the star tracker measurements are on the order of several arc minutes. The star tracker and gyro measurements are combined in a Kalman-based attitude estimator, which accounts for the Earth's rate of rotation, to obtain attitude knowledge precise to the sub-arc minute-level.

For a formation to couple translational degrees-of-freedom, spacecraft must estimate relative positions. Relative position knowledge can be obtained from direct relative measurements or by differencing positions with respect to a common reference point. Communicating and differencing GPS-derived positions is an example of the latter (Ref. 16). An example of direct sensing is a camera that measures relative bearing by the location of an image on a CCD and relative range by the size of the image (Ref. 17).

The FCT uses sensors of both types. First, as discussed previously, the FCT star tracker also measures a robot's position in the FCT Room Frame. This type of measurement is equivalent to a GPS measurement. The star tracker position measure-

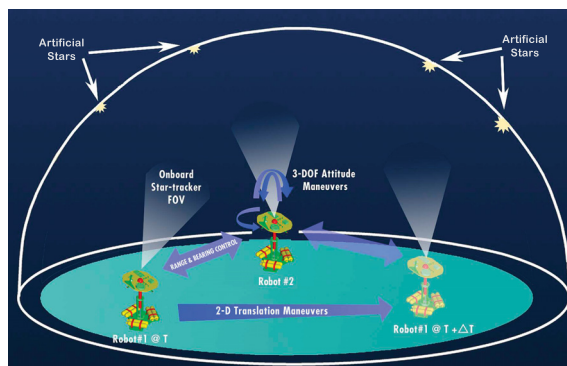


Figure 4. Principle of Operation for Pseudo-Star Trackers. Since artificial stars are in the near-field, the star tracker provides both translational and rotational measurements.

ment is precise to the sub-centimeter level. To function as a formation sensor, the SEs on each robot read the pseudo-GPS measurement from the avionics and broadcast it. The SEs then difference their local measurements with the broadcast measurements and pass this relative measurement to the FACS. The differenced measurement has centimeter-level precision. This SE interface emulates omni-directional sensors for deep space formations, such as the Formation Acquisition Sensor (FAS) (Ref. 18).

The direct relative sensor for the FCT, shown in Figure 5, is called the Optical Pointing Loop (OPL). The OPL is based on a laser shear sensor co-sighted with a laser range finder. Conceptually, a laser diode, fast steering mirror (FSM), and position sensing device (PSD) on one spacecraft are used to keep the laser diode output centered within a corner cube mounted on another spacecraft. The relative bearing is then given by the angular position of the FSM. A co-sighted SICK DML40-1111 laser range finder provides relative range. The FSM is from Left Hand Design Corporation and was developed under an SBIR as part of the StarLight Project. The OPL will measure range to a precision of several millimeters and bearing to tens of arc seconds. The OPL is planned for installation in early 2008.

Two key services provided by the SE are spacecraft-to-spacecraft clock offset estimation and control cycle synchronization. Knowledge of clock offsets is necessary for processing communicated measurements in formation estimators. Control cycle synchronization, which is the process of making control cycles on separate spacecraft start at the same times, is required for the highest precision formation control. During operation, the SE keeps control cycles synchronized to the millisecond-level. The SE also hosts the Inter-Spacecraft Communication (ISC) manager. Currently, a time division multiple access (TDMA) architecture is implemented for sharing the wireless links between ISC, uplink and

downlink, clock offset estimation, and control cycle synchronization. Communication protocols such as TCP and UDP are not satisfactory since TCP can disrupt real-time performance and UDP is not robust to packet drops. A new protocol was developed called Real-Time UDP that adds timeouts and a limit to packet resends.

### 3. FORMATION ROTATION G&C

Having reviewed the FCT, now the specific maneuver being demonstrated is discussed, including the on-board algorithm that generates the formation trajectories that the robots follow in real-time and the feedback control loops used to do so.

#### 3.1. Maneuver Specification

The design of TPF-I has evolved through various planar configurations to the current tetrahedral configuration. In each design, however, the formation must rotate as a virtual rigid body about the bore-sight of the synthetic aperture. This rotation axis is perpendicular to the plane defined by the collecting spacecraft (collectors). The location of the rotation axis with respect to the collector-plane is free and is generally chosen based on a metric of fuel optimality.

Another constraint can be imposed depending on the type of translational actuation. For pulse-width modulated (PWM) thrusters, the resulting impulse can cause optical control loops within the interferometric payload to temporarily stop tracking. Hence, thruster quiescent windows must be enforced during which science data is collected. Then, after a window with thruster firings, the payload loops reacquire during the next quiescent window and science data is collected again. The thruster-firing windows must be synchronized across the formation. If reaction wheel-induced vibrations will also cause loss of track, then all degrees-of-freedom must be controlled on thrusters in these thruster-firing windows.

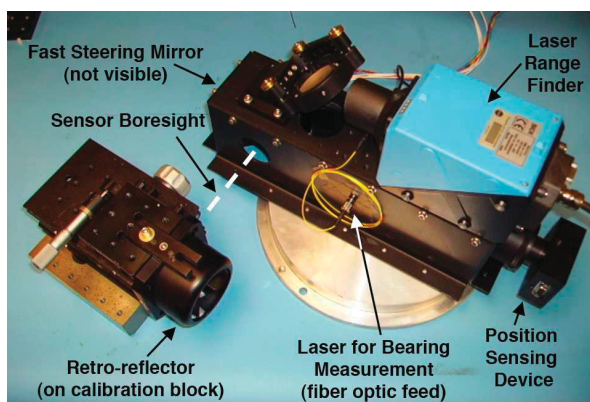


Figure 5. The Optical Pointing Loop for Direct Relative Sensing in the FCT.

Due to this quiescence constraint, the spacecraft travel on polygonal approximations to circles. The periodic thruster firings direct the spacecraft onto the next side of the polygon. Also, even if throttleable thrusters, such as ion thrusters, are used, the finite duration of the digital control cycle results in spacecraft traveling on a polygon as well. In this case, of course, the polygonal approximation is much finer. For either type of thruster, the polygonal approximation may be characterized by the angular chord width  $\theta$ . See Figures 6 and 7.

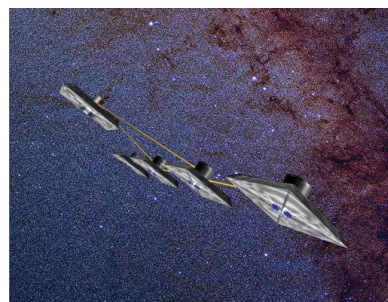


Figure 6. TPF-I Linear Array.

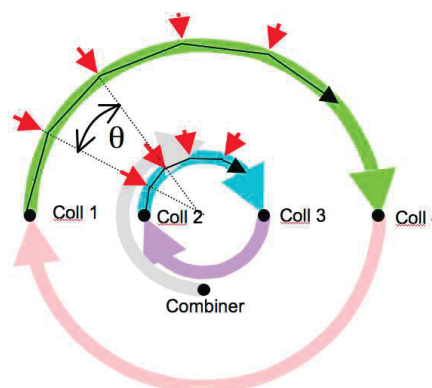


Figure 7. Example of Polygonal Approximations in Formation Rotation of TPF-I Linear Array. Arrows indicate thruster firing windows. “Coll” stands for collector spacecraft.

Five parameters specify a formation rotation: angular chord width  $\theta$ , rotation axis  $\lambda$ , rotation rate  $\omega$ , rotation angle  $\phi$ , and vehicle separation  $b$  (for baseline). The values of these parameters for FCT demonstrations are derived from the TPF-I Technology Roadmap, testbed requirements levied during the FCT development reviews, and system-level error budgets. The FCT rotation requirements are given in Table 1.

An example maneuver with  $\theta = 40$  deg. is shown in Figure 8. There is a transient spin-up regime and a performance regime. The performance regime consists of one chord plus a quarter chord on either side. The performance regime shows that the formation can transition between chords while maintaining performance. Additionally, the white thruster clusters on each robot, which lie on the initial inter-robot vec-

tor, must remain pointed at the other robot. That is, the robots translate and rotate in synchrony.

Table 1. FCT Formation Rotation Requirements.

Parameter	Value	Note
$\theta$	20, 40 deg.	To show flexibility
$\lambda$	[0 0 1]	FCT currently 5DOF
$\omega$	5 arcmin/s	10x flight rate
$\phi$	90 deg.	Per Tech. Roadmap
$b$	3.4 m	From error budgets

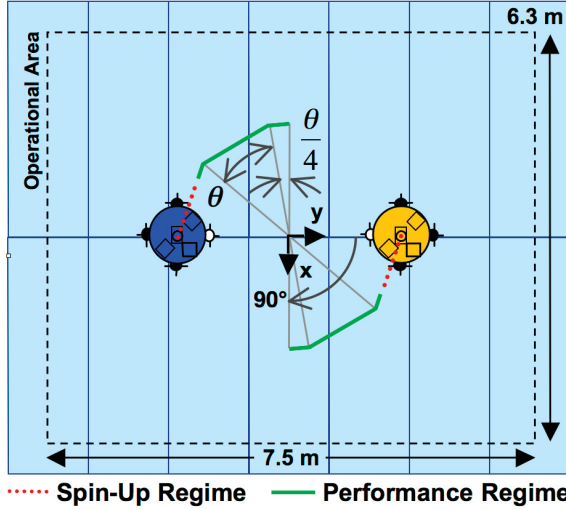


Figure 8. Schematic of formation rotation in the FCT with parameters of Table 1.

### 3.2. Rotation Guidance Algorithm

To show a system-level capability, the FCT robots must be commanded and operated as a formation. In particular, a single high-level command initiates autonomous, on-board path-planning and execution of a formation rotation. Except for the baseline  $b$ , this command specifies the parameters of Table 1. The baseline for a formation rotation is the current stored baseline value. The baseline value is updated by commanding a formation reconfiguration, which moves spacecraft from one static configuration to another along collision-free trajectories. An example command for a synchronized rotation is

```
facs_cmd GUID_FORM_SYNC_ROT time {450}
Rotation {0.0,0.0,-2.0944} Duration {1440}
LinArcLen {0.6982}
```

A TCL-based interpreter in the SEs processes this command: `facs_cmd` is a keyword for this interpreter, `GUID_FORM_SYNC_ROT` is a keyword for the sub-interpreter within the guidance software module, `time` specifies the rotation start time, `Rotation` is  $\phi \cdot \lambda$ ; `LinArcLen` is  $\theta$ , and `Duration` is  $\phi/\omega$ .

The formation synchronized rotation guidance algorithm is discussed more fully in (Ref. 13). Figures

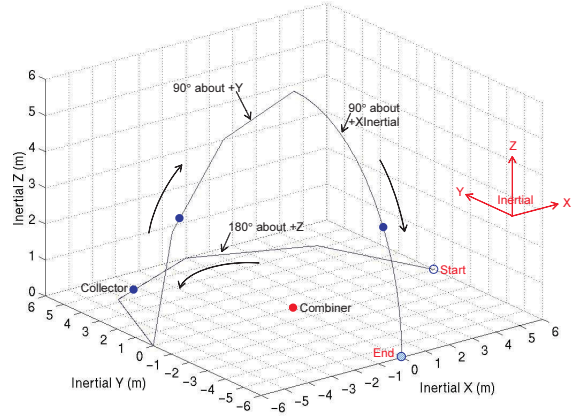


Figure 9. Example Formation Rotation Maneuvers.

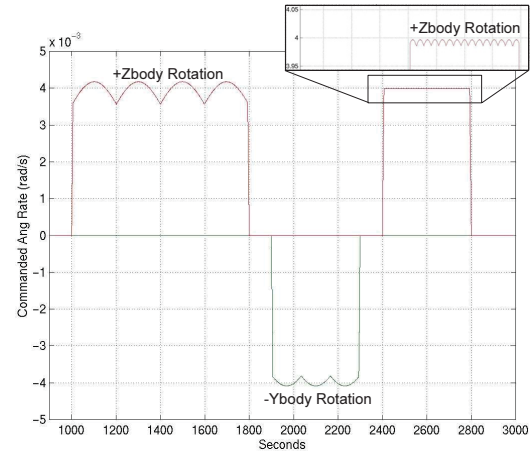


Figure 10. Corresponding Angular Rate Command for Example Formation Rotation Maneuvers. Angular rate commands are based on attitude commands.

9 and 10 show example 6DOF guidance output—the reference signal for the control loops—for several example rotations. Observe that the angular rate commands peak midway along chords, as is needed to maintain body-fixed vectors aligned with relative position vectors. Intuitively, since the spacecraft are “cutting corners” and so traveling faster than spacecraft following a circle, they must turn faster to rotate the same amount as a circle-traveling spacecraft.

### 3.3. Formation Control Architecture

For small-to-medium formations, the Leader/Follower (L/F) formation architecture is effective (Ref. 9). In L/F, the control couplings among spacecraft in a formation are hierarchical. Each follower spacecraft, which can also be a leader for another, controls with respect to a subset of other vehicles. This subset typically contains only one craft. Necessarily, there is at least one spacecraft that follows no one. The hierarchical structure leads to straightforward stability conditions based on the stability of a follower’s tracking law. For the

Table 2. Summary of FCT Synchronized Formation Rotation Demonstrations.

Date <sup>a</sup>	$\theta$ , deg.	Leader Attitude			Follower Attitude			Follower Position	
		Error RMS, arcmin			Error RMS, arcmin			Error RMS, cm	
		x	y	z	x	y	z	x	y
9/24/07 10:48 am	40	2.6292	2.9554	1.7550	5.6972	5.7259	3.2233	2.4597	4.2836
9/26/07 10:04 pm	40	2.6684	2.7428	2.0424	4.5038	6.1762	2.9509	2.5953	4.7505
10/02/07 3:11 pm	40	2.3876	2.4186	1.9105	5.7187	6.6255	3.0635	2.3935	4.9667
9/18/07 7:55 pm	20	2.2925	2.3929	1.9620	4.4459	6.3579	3.6195	1.4911	4.4580
9/21/07 12:45 pm	20	3.1281	3.4893	1.8404	4.6419	6.2720	3.1065	1.4286	2.3877
9/25/07 10:43 am	20	2.6648	2.9348	1.6700	4.7741	5.1391	2.7042	1.3880	2.4101

<sup>a</sup>Data convention is month/day/year.

current two robots of the FCT, an L/F architecture is implemented in the FACS. The Follower controls its position relative to the Leader, and the Leader applies feedforward forces.

### 3.4. Formation Drift Controller

Formation control is concerned with relative positions. An additional, outer control loop is needed for the inertial position of a formation. For example, for a formation in LEO, the formation control loop would maintain, say, a tetrahedral configuration, while an outer orbit control loop maintains the overall orbit of the formation. This outer loop in the FCT is called the Formation Drift Controller (FDC). It is a low-authority controller that maintains the geometric center of the formation at a specified point within the FCT. To prevent interference with the formation control loops, a single robot collects inertial position data, determines a translational impulse to apply to the formation, and broadcasts this impulse to all formation members. Then the robots execute the impulse simultaneously. Since the same impulse is applied simultaneously by all formation members, the relative position dynamics—that is, the formation dynamics—are not affected.

## 4. FCT DEMONSTRATIONS

For each demonstration, the robots are maneuvered independently to starting positions and shut-down. Then the robots are re-started and go through their single-spacecraft check-out modes. During these check-outs, a command script is sent to each robot. After these check-outs, each robot has established inertial attitude control and independent, inertial position control using their gyros and star trackers. The command for formation initialization then activates. During formation initialization, independent, inertial translational control loops are disabled, the robots establish communication, synchronize control cycles, and point specified body vectors, which correspond to payload or eventual inter-robot sensor pointing requirements, at one another. At the end of formation initialization, the robots automatically reconfigure to their current configuration which activates the formation control loop. Then the command for formation rotation activates. Beginning at the end of

formation initialization, the relative position is fed back for formation control.

Table 2 summarizes the results from the demonstrations and Figures 11-16 show the results in detail for the demonstration run on 9/21/07. All data reported is telemetry downlinked from the robots. The single exception is the floor height data in Figure 16, which was obtained from a laser survey. The data in Table 2 consists of the error RMS's over a performance regime. When multiple performance regimes occur in a run, such as when  $\theta = 20$  deg., the regime with the best performance was selected. From the dates in Table 2, it can be seen that each demonstration for a specific  $\theta$  occurred at least two days after the previous one. All runs meet the requirements of 6.67 arcmin RMS by axis in attitude and 5.0 cm RMS by axis in relative position.

Figures 11-16 show data from approximately 60 degrees (12.5 minutes) of the demonstration run on 9/21/07. The Leader attitude performance is approximately 40% better than the Followers due to residual, uncalibrated thruster misalignments. Since the Follower thrusts for both attitude and formation control, these misalignments have a greater effect. The gains of the formation control loop were increased until attitude performance neared its limit. Since the 40 deg. chords had longer performance regimes, more relaxed relative position control was necessary to meet the attitude performance requirements. More precise formation control is possible. Nonetheless, Figure 13 shows that essentially  $\pm 5$  cm can be achieved on the ground. Figure 16 superimposes the inertial motion of the robots on a topographic map of the FCT precision flat floor.

## 5. SUMMARY AND FUTURE WORK

An initial robust capability for precision synchronized formation rotations has been demonstrated for two vehicles in the Formation Control Testbed (FCT). Six demonstrations were performed over the course of two weeks for two different guidance profiles. The different profiles resulted from variations in the command parameters sent to the robots: the same Formation and Attitude Control System (FACS) was exercised in every case. All guidance, estimation, and control functions were performed on-

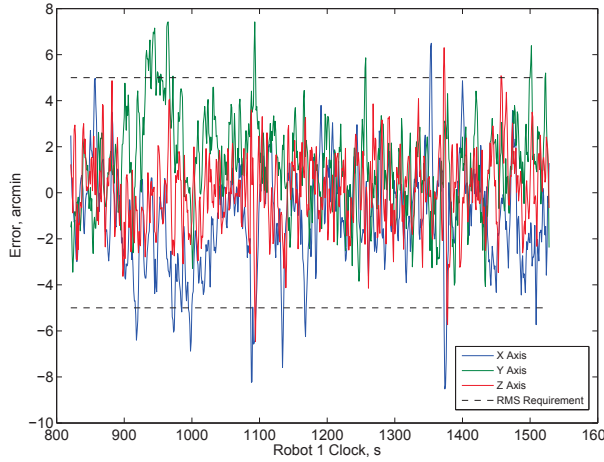


Figure 11. Leader Attitude Error for 9/21/07.

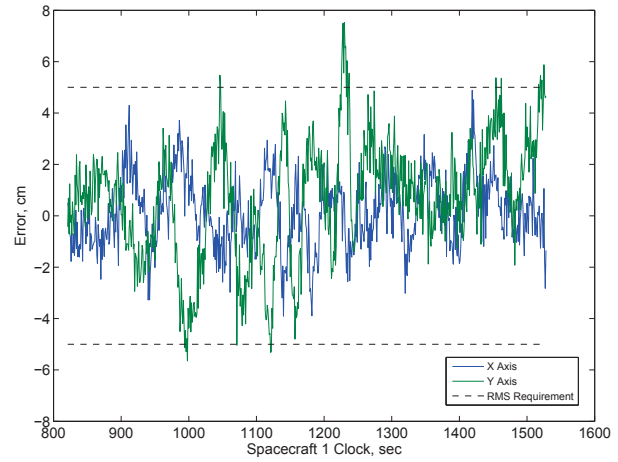


Figure 13. Relative Position Error for 9/21/07.

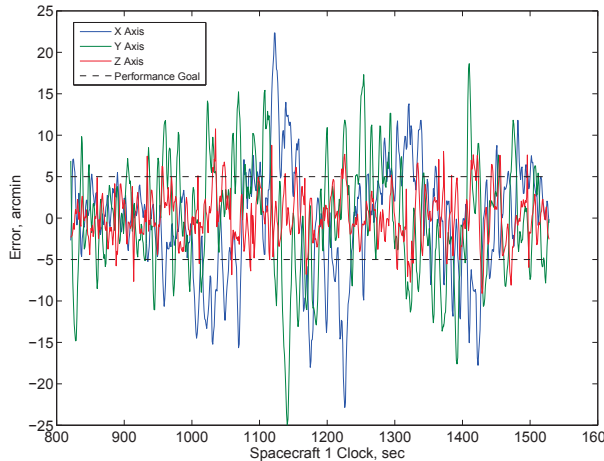


Figure 12. Follower Attitude Error for 9/21/07.

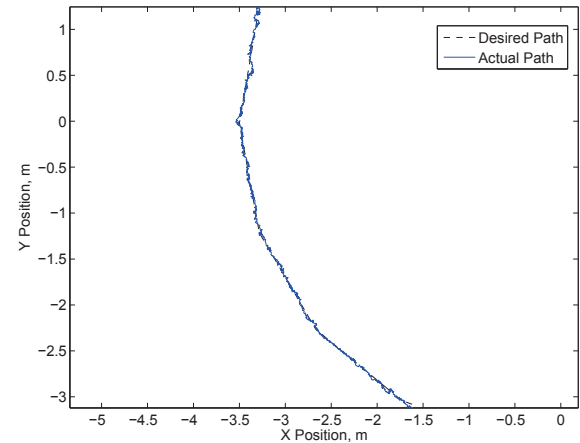


Figure 14. Relative Position Compared to Guidance Command for 9/21/07. Four chords are visible.

board the robots and cued by commands uplinked to the robots. The robots communicated, synchronized control cycles, and autonomously executed high-level commands. Further, per the definition of a formation in the Introduction, the synchronized rotation was executed as a formation maneuver: in this case, the relative position was continually fed back to couple the robots. The 6DOF maneuver commands were executed to 6.67 arcmin RMS by axis in attitude and 5 cm RMS by axis in relative position. The majority of cases performed to  $\pm 8$  cm in relative position. The limiting factor in 6DOF performance was the balance between integrator rise-time in the relative position control loops and the resulting reduction in attitude performance due to residual thruster misalignments.

The FCT was discussed in detail, and while currently 5DOF, the sixth degree of freedom is currently being installed. See Figure 15, which shows the Vertical Stage for one of the robots. The second vertical stage will be installed in March 2008. In addition, the Op-

tical Pointing Loop (OPL), which will provide direct relative sensing and is shown in Figure 5, is nearing completion. Future goals include demonstrating precision, synchronized maneuvers with more vehicles and with direct relative sensing, thereby allowing for multiple, simultaneous levels of formation sensing as will be the case for flight missions. Upon demonstration of sufficiently complex, nominal formation maneuvers, fault detection and recovery capabilities must be demonstrated. In a sense, a formation is only as good as its collision avoidance.

## ACKNOWLEDGMENTS

This research was performed at the Jet Propulsion Laboratory, California Institute of Technology, under contract with the National Aeronautics and Space Administration. The authors gratefully acknowledge Yan Brenman, Arin Morfopoulos, Ali Vafaei, and Charles Bergh, all of JPL, who contributed to the success of this effort.

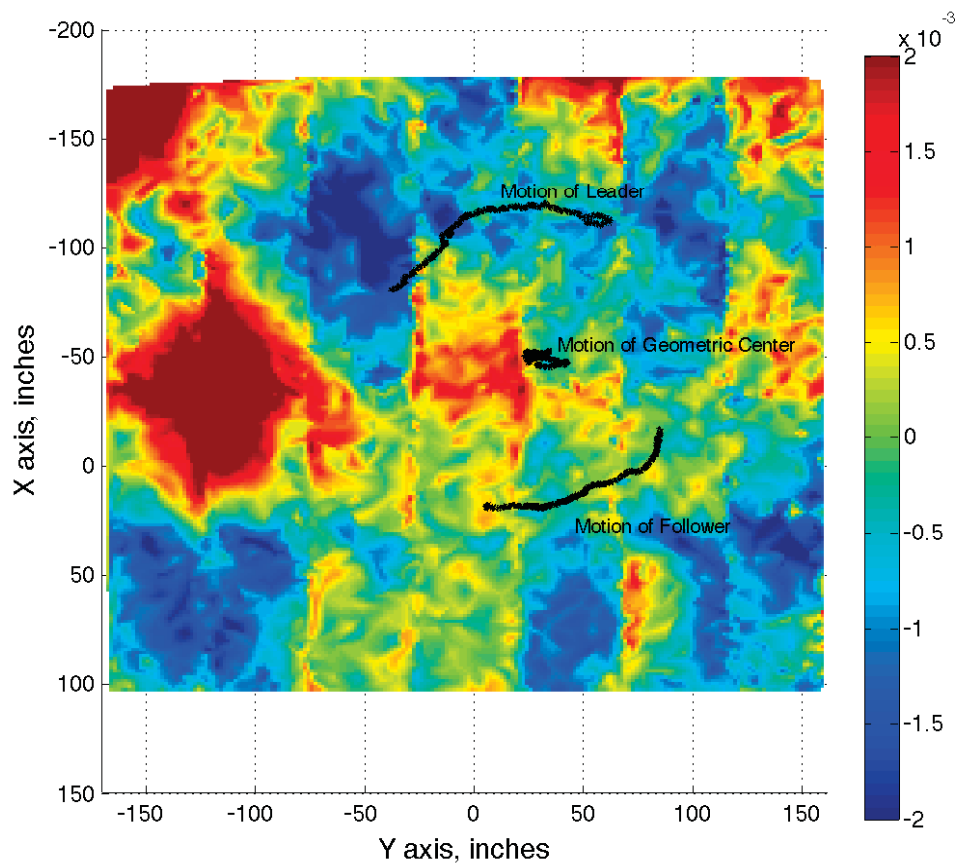


Figure 16. Inertial Motion of FCT Robots During Demonstration of 9/21/07 Superimposed on Topographic Map of FCT Precision Flat Floor. Height variations are  $\pm 0.002$  inches. Additionally, panel edges can be discerned. The robot trajectories traverse multiple panels.

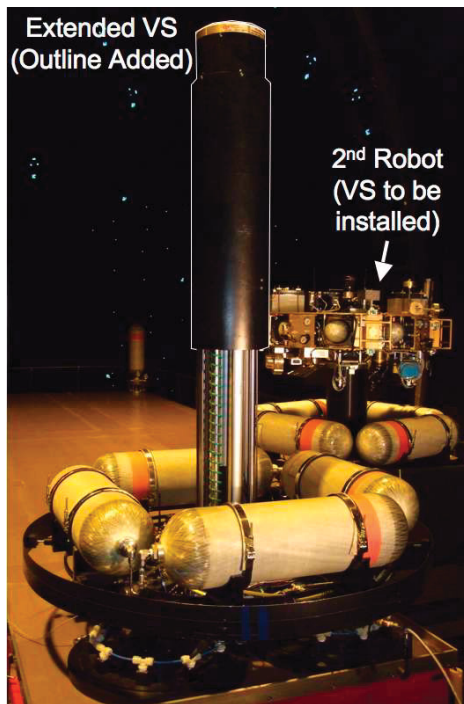


Figure 15. Installation of Vertical Stage on Translational Platform of an FCT Robot.

## REFERENCES

1. Lawson, P.R. and Ahmed, A., Gappinger, R., Ksendzov, A., Lay, O., Martin, S., Peters, R., Scharf, D., Wallace, J., and Ware, B. Terrestrial Planet Finder Interferometer technology status and plans. In Monnier, J., Schöller, M., and Danchi, W., editors, *Proc. SPIE Vol. 6268: Adv. Stellar Interferometry*, pages 626828.1–8, 2006.
2. Fridlund, C. and Gondoin, P. Darwin mission. In Shao, M., editor, *Interferometry in Space, SPIE Vol. 4852*, pages 394–404, 2003.
3. Das, A. and Cobb, R. TECHSAT 21 - A revolutionary concept in distributed space based sensing. In *AIAA Defense and Civil Space Programs Conf.*, Huntsville, AL, 1998.
4. Gendreau, K., Cash, W., Shipley, A., and White, N. The MAXIM pathfinder X-ray interferometry mission. In Truemper, J. and Tananbaum, H., editors, *Proc. of SPIE Vol. 4851: X-Ray and Gamma-Ray Telescopes and Instruments for Astronomy*, pages 353–364, 2003.
5. Bristow, J., Folta, D., and Hartman, K. A formation flying technology vision. In *Proc. AIAA Space Conf.*, Long Beach, CA, 2000.
6. Lay, O., Gunter, S., Hamlin, L., Henry, C., Li, Y.-Y., Martin, S., Purcell, G., Ware, B., Wertz, J., and Noecker, M. Architecture trade study for the the Terrestrial Planet Finder Interferometer. In Coulter, D., editor, *Proc. SPIE Vol. 5905: Techniques and Instrumentation for Detection of Exoplanets II*, pages 590502.1–13, 2005.
7. Cash, W., Schindhelm, E., Arenberg, J., Polidan, R., Kilston, S., and Noecker, C. The New Worlds Observer: using occulters to directly observe planets. In Mather, J., MacEwen, H., and de Graauw, M., editors, *Proc. SPIE Vol. 6265: Space Telescopes and Instrumentation I: Optical, Infrared, and Millimeter*, pages 6265.V1–11, 2006.
8. Scharf, D., Ploen, S., and Hadaegh, F. A survey of spacecraft formation flying guidance and control (Part I): Guidance. In *Proc. Amer. Contr. Conf.*, Denver, CO, 2003.
9. Scharf, D., Hadaegh, F., and Ploen, S. A survey of spacecraft formation flying guidance and control (Part II): Control. In *Proc. Amer. Contr. Conf.*, Boston, MA, 2004.
10. Lawson, P. and Dooley, J. Technology plan for the terrestrial planet finder interferometer. JPL Publication 05-5, Jet Propulsion Laboratory, California Institute of Technology, Pasadena, CA, USA, 2005. Available online at <http://planetquest.jpl.nasa.gov/Navigator/library/tpf1414.pdf>.
11. Regehr, M., Acikmese, A., Ahmed, A., Aung, M., Clark, K., MacNeal, P., Shields, J., Singh, G., Bailey, R., Bushnell, C., Hicke, A., Lytle, B., and Rasmussen, R. The Formation Control Testbed. In *Proc. IEEE Aerospace Conf.*, pages 557–564, Big Sky, MT, 2004.
12. Scharf, D., Hadaegh, F., Keim, J., Benowitz, E., and Lawson, P. Flight-like ground demonstration of precision formation flying spacecraft. In Coulter, D., editor, *Proc. SPIE Vol. 6693: Techniques and Instrumentation for the Detection of Exoplanets III*, pages 669307.1–12, 2007.
13. Scharf, D., Hadaegh, F., Rahman, Z., Shields, J., Singh, G., and Wette, M. An overview of the formation and attitude control system for the terrestrial planet finder interferometer. In *Proc. 2nd Int. Symp. on Formation Flying Missions & Technologies*, Washington, D.C., 2004.
14. Wette, M., Sohl, G., Scharf, D., and Benowitz, E. The formation algorithms and simulation testbed. In *Proc. 2nd Int. Symp. on Formation Flying Missions & Technologies*, Washington, D.C., 2004.
15. Shields, J. The Formation Control Testbed Celestial Sensor: Overview, modelling, and calibrated performance. In *Proc. IEEE Aerospace Conf.*, Big Sky, MT, 2005.
16. Ruth, M. and Tracy, C. Video-guidance design for the DART rendezvous mission. In Tchoryk,

- Jr., P. and Wright, M., editors, *Proc. SPIE Vol. 5419: Spacecraft Platforms and Infrastructure*, pages 92–106, 2004.
17. Weismuller, T. and Leinz, M. GN&C technology demonstrated by the Orbital Express Autonomous Rendezvous and Capture Sensor System. In Jolly, S. and Culp, R., editors, *Adv. Astro. Sciences Vol. 125: Guidance and Control 2006*, 2006.
  18. Purcell, G., Tien, J., Young, L., and Srinivasan, J. Formation acquisition sensor for the Terrestrial Planet Finder mission. In *Proc. IEEE Aerospace Conf.*, Big Sky, MT, 2004.